

# Theory of Andreev resonances in quantum dots

N R Claughton, M Leadbeater and C J Lambert

School of Physics and Chemistry, Lancaster University, Lancaster LA1 4YB, UK

Received 2 August 1995, in final form 4 September 1995

**Abstract.** We present a comprehensive theory of the electrical conductance  $G$  of phase-coherent, multi-channel, resonant structures in the presence of superconductivity. When voltages of the order of the level spacing are applied, particle-hole symmetry is broken and our results differ significantly from earlier descriptions. After deriving generalizations of the well-known Breit-Wigner formula, valid in the presence of superconductivity, results for resonant transport in three classes of structure are obtained. First, for a superconducting dot (SDOT) connected to normal contacts (N), we examine the change in conductance as the magnitude of the superconducting order parameter increases from zero. The change is typically negative, except near a normal-state resonance, where large positive changes can occur. Secondly, for a structure comprising a normal (N) contact, a normal dot (NDOT) and a superconducting (S) contact, we predict that finite-voltage, differential conductance resonances are strongly suppressed by the switching on of superconductivity in the S contact. In the weak-coupling limit, resonances which survive have a double-peaked line-shape. Thirdly, analytic results are presented for superconductivity-enhanced, quasi-particle interferometers (SEQUINs), which demonstrate that resonant SEQUINs can provide galvanometric magnetic flux detectors, with a sensitivity in excess of the flux quantum.

## 1. Introduction

Recent advances in the fabrication of nanoscale structures have led to increasing interest in transport through resonant tunnel junctions and quantum dots [1, 2]. In part this is due to the new physics associated with Coulomb blockade [3] and in part due to growing interest in quantum chaos [4–7]. The bulk of work in this area has focused on normal structures, but more recently attention has turned to hybrid structures involving a superconducting component. Recently it has been demonstrated experimentally that the energy gap of a superconducting dot is directly observable through Coulomb blockade experiments [8] and theoretical work on incoherent transport through such dots has been carried out [9]. In this paper, we present a detailed description of the effect of superconductivity on phase-coherent transport through resonant structures, in the limit where charging effects can be ignored. This limit should be experimentally accessible, because even intimate contact with a superconductor will not broaden states below the gap. Many new phenomena involving coherent transport through resonant superconducting hybrids are expected to manifest themselves in a small number of generic structures. One such example is a ‘N–NDOT–S’ structure comprising one or more normal (N) current-carrying leads, in contact with a normal zero-dimensional ‘dot’ (NDOT), which in turn makes contact with a superconducting (S) lead. In contrast with the zero-voltage limit, where a general multi-channel description of this structure is available [10], there currently exists only a single one-dimensional study of finite-voltage, resonant transport [11], in which a  $\delta$ -function potential well, with a single localized state, is introduced into a one-dimensional insulating barrier.

To understand the new physics likely to emerge in such a structure, it is useful to recall the known properties of a N-NDOT-N' system, in which excitations incident from normal contacts (N, N') can resonantly tunnel through the NDOT. In this case the zero-temperature electrical conductance is  $G = (2e^2/h)T_0$ , where  $T_0$  is the normal transmission coefficient through the device. When contact is made with lead N (N'), the levels of the NDOT are broadened by an amount  $\Gamma$  ( $\Gamma'$ ) and, 'on-resonance',  $T_0$  is given by the Breit-Wigner formula [12, 13]

$$T_0 = 4\Gamma\Gamma'/(\Gamma + \Gamma')^2. \quad (1.1)$$

The statistical properties of these resonant values of  $G$  are determined by those of  $\Gamma$  and  $\Gamma'$ , which in turn depend on the values of the wavefunctions of the resonant level at the contacts. It is here that ideas originating from studies of quantum chaos can be used to yield general predictions about statistical properties [4-7]. In contrast with equation (1.1), the sub-gap, zero-temperature electrical conductance of a N-NDOT-S structure is given by the Blonder, Tinkham and Klapwijk (BTK) formula [14]  $G = (2e^2/h)2R_a$ , where  $R_a$  is the probability that an excitation incident from N will Andreev reflect from the NDOT-S composite scatterer. For energies less than the superconducting energy gap  $\Delta_0$ , levels are broadened only by the N-NDOT contact. For charge transport to occur, an electron from the N lead must normally transmit into the NDOT (with probability proportional to  $\Gamma_+$ ), normally transmit into S (with probability  $\sigma'_{+-}$ ) and Andreev convert into a hole. The hole must then enter the dot (with probability  $\sigma'_{-+}$ ) and finally exit into the N lead (with probability  $\Gamma_+$ ). The resulting analogue of the Breit-Wigner formula for  $R_a$  is of the form [10]

$$R_a = 4[\Gamma_+^2\sigma'_{+-}\sigma'_{-+}]/[\Gamma_+^2 + \sigma'_{+-}\sigma'_{-+}]^2. \quad (1.2)$$

For a normal system described by equation (1.1),  $G$  is a maximum when

$$\Gamma = \Gamma'. \quad (1.3)$$

For a system described by equation (1.2),  $G$  is a maximum when

$$\Gamma_+^2 = \sigma'_{+-}\sigma'_{-+}. \quad (1.4)$$

Hence resonances are predicted [10] to persist when superconductivity is switched on, with a probability comparable with that of the normal state. In section 6 (below), we present a detailed analysis of multi-channel resonant transport, which confirms this zero-voltage prediction, but which also contains the surprising prediction that resonances in the finite-voltage differential conductance are *destroyed* by superconductivity. Furthermore, in contrast with single-peaked resonances predicted in [10], finite-voltage resonances which do survive can have a twin-peaked structure.

A second class of structures involves two (or more) separate superconductors S and S', with respective order parameter phases  $\phi$ ,  $\phi'$ . The resonant energies of a N-SS' or N-NDOT-SS' composite will vary periodically with the phase difference  $\phi - \phi'$  [15-22] and one expects novel features to appear, not yet observed in the small number of Andreev interference experiments carried out to date [23-26]. Depending on the particular geometry, quasi-particle interference effects can be significantly enhanced by the presence of superconductivity and in section 7, generic properties of such superconductivity-enhanced, quasi-particle interferometers (SEQUINs) are highlighted.

A third class of generic structures is formed when a normal lead makes contact with a superconducting dot (SDOT), which in turn makes contact with a second normal lead. It is known [27, 28] that when a superconducting island is added to a normal host, the electrical conductance can either increase or decrease, depending on the microscopic configuration of host impurities. This prediction has been confirmed experimentally in metallic samples [29, 30], but the role of resonances remains to be clarified. For a N-SDOT-N' structure, the BTK formula [14] for  $G$  does not apply and more general current-voltage relations [31–33] involving normal and Andreev transmission probabilities must be used. In what follows, after deriving Breit-Wigner analogues for these quantities, we obtain analytic results for the change in conductance due to the switching on of superconductivity in a resonant dot.

For simplicity, we restrict the following analysis to structures for which well-defined dc transport measurements exist and therefore do not discuss Josephson junctions formed from S-NDOT-S' structures [34–37]. In appendix A, a general approach to finite-voltage transport through phase-coherent structures is discussed, and in section 2, an analogue of the Breit-Wigner formula for arbitrary phase-coherent structures is derived. In section 3, these sections are combined to yield general results for resonant transport in the presence of Andreev scattering. In sections 4 and 5, analytic results for N-SDOT-N and N-NDOT-S structures are presented and in section 6, generic properties of resonant SEQUINs are described. Finally in section 7, analytic predictions are compared with the results of exact numerical solutions of the Bogoliubov-de Gennes equation in two dimensions.

## 2. Analysis of phase-coherent, resonant transport

In this section we derive an expression for the quasi-particle scattering amplitude  $s_{n,n'}(E, H)$  and transmission coefficient  $T_{nn'} = |s_{n,n'}(E, H)|^2$  between two scattering channels  $n, n'$  of an open vector space  $A$ , in contact with a sub-space  $B$ . These quantities are functions of the quasi-particle energy  $E$  and the Hamiltonian  $H$  of the combined structure and, as discussed in appendix A, underpin various conductance formulae derived in subsequent sections. The result is very general and makes no assumptions about the presence or otherwise of resonances. More precisely, we describe a quantum structure connected to ideal, normal leads of constant cross-section, labelled  $L = 1, 2, \dots$  and therefore begin by considering two vector spaces  $A$  and  $B$ , spanned by a set of basis functions. In what follows, the sub-space  $B$  represents the structure of interest and sub-space  $A$  the normal leads, as shown in figure 1. The Hamiltonian is  $H = H_A + H_B + H_1$ , where  $H_1$  allows transitions between the sub-spaces. Since  $H_1$  can be written

$$H_1 = \begin{pmatrix} 0 & W \\ W^\dagger & 0 \end{pmatrix} \quad (2.1)$$

the Green's function  $G$  for the combined space  $A \oplus B$  has the form

$$G = \begin{pmatrix} G_{AA} & G_{AB} \\ G_{BA} & G_{BB} \end{pmatrix}. \quad (2.2)$$

For  $n \neq n'$ , the result, which we derive for normal leads described by a real Hamiltonian, is

$$T_{nn'} = 4 \text{Trace} [\Gamma(n)G_{BB}\Gamma(n')G_{BB}^\dagger] \quad (2.3a)$$

and for  $n = n'$  is

$$T_{nn} = |1 - 2i \text{Trace} [\Gamma(n)G_{BB}]|^2 \quad (2.3b)$$

where

$$G_{BB}^{-1} = g_B^{-1} - \sigma' - \sigma + i\Gamma \quad (2.4)$$

and the trace is over all internal levels of  $B$ . In these expressions,  $\Gamma(n)$  is a Hermitian matrix of inverse lifetimes,  $\Gamma = \sum_n \Gamma(n)$ ,  $\sigma$  and  $\sigma'$  are Hermitian self-energy matrices and  $g_B$  is the retarded Green's function of sub-space  $B$  when  $H_1 = 0$ . The above result has been cast in a form which resembles the Breit-Wigner formula, but is very general and makes no assumptions about the presence or otherwise of resonances.

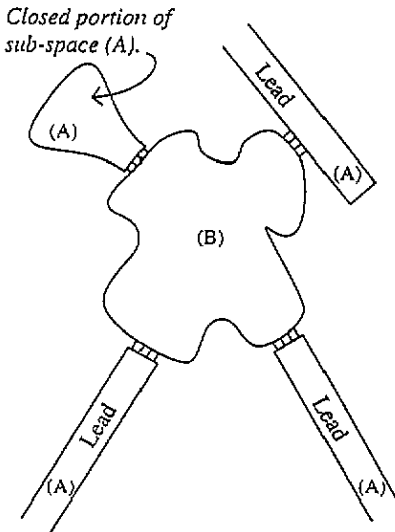


Figure 1. A sketch of a closed sub-space  $B$ , in contact with an open sub-space  $A$ .

The form of equations (2.3) and (2.4) highlights the essential difference between open and closed channels. In the absence of open channels,  $\sigma$  and  $\Gamma$  are identically zero and if the sub-space  $B$  is closed,  $G_{BB}$  describes a quantum structure with well-defined energy levels, shifted by the self energy  $\sigma'$  arising from contact with closed channels. Clearly no quasi-particle transport is possible through such a structure. When contact is made with open channels, the levels are further shifted by the self-energy matrix  $\sigma$  and more crucially are broadened by the lifetime matrix  $\Gamma$ . If the sub-space  $B$  is closed, it can be shown that equations (2.3) satisfy

$$\sum_n T_{nn'} = \sum_n T_{n'n} = 1.$$

During the past decade, the Breit-Wigner formula [12, 13] has been applied to a variety of problems involving resonant transport in normal-state structures, including normal-metal rings [42], quantum Hall structures [43] and, more recently, Fano resonances in quasi-one-dimensional wires [44]. For a normal-metallic conductor, under resonant conditions, where the level spacing is much greater than the broadening, Büttiker has presented a multi-channel

derivation of the Breit–Wigner formula through a single resonant level [45]. This limit is recovered from equation (2.3) by restricting the trace to a single level. In what follows, we shall encounter situations in which, due to particle–hole symmetry, degenerate states can simultaneously resonate, and therefore the more general formulae (2.3) is required.

To derive this result, we recall that when  $H_1 = 0$ ,  $G$  reduces to the Green’s function  $g$  of the decoupled system, where

$$g = \begin{pmatrix} g_A & 0 \\ 0 & g_B \end{pmatrix} \quad (2.5)$$

and noting that  $G = g(1 - H_1 g)^{-1}$  yields

$$\begin{pmatrix} G_{AA} & G_{AB} \\ G_{BA} & G_{BB} \end{pmatrix} = \begin{pmatrix} g_A(1 - W g_B W^\dagger g_A)^{-1} & g_A(1 - W g_B W^\dagger g_A)^{-1} W g_B \\ g_B(1 - W^\dagger g_A W g_B)^{-1} W^\dagger g_A & g_B(1 - W^\dagger g_A W g_B)^{-1} \end{pmatrix}. \quad (2.6)$$

Rewriting the above result for  $G_{AA}$  in the form

$$G_{AA} = g_A + g_A W g_B (1 - W^\dagger g_A W g_B)^{-1} W^\dagger g_A \quad (2.7)$$

yields

$$G_{AA} = g_A + g_A W G_{BB} W^\dagger g_A \quad (2.8)$$

$$G_{AB} = g_A W G_{BB} \quad (2.9)$$

and

$$G_{BA} = G_{BB} W^\dagger g_A. \quad (2.10)$$

These demonstrate that once  $G_{BB}$  is known, all other quantities are determined. To obtain an expression for transmission coefficients we introduce a set of states  $\{|\bar{n}\rangle\}$ , which span the sub-space  $A$ , and write  $g_A = \sum_{\bar{n}\bar{m}} |\bar{n}\rangle g_{\bar{n}\bar{m}} \langle \bar{m}|$ . Since part of  $A$  consists of a number of ideal, straight, normal leads of constant cross-section, described by a real Hamiltonian, it is convenient to associate a sub-set of the states  $\{|\bar{n}\rangle\}$  with open channels of these leads. For these states, we introduce the notation  $|\bar{n}\rangle = |n, x\rangle$ , where  $n$  is a discrete label identifying the lead, quasi-particle-type, transverse kinetic energy and any other quantum numbers of an open channel, and  $x$  is a position coordinate parallel to the lead. With this notation,

$$g_A = \sum_{n,x,x'} |n, x\rangle g_n(x, x') \langle n, x'| + \sum'_{\bar{n}\bar{m}} |\bar{n}\rangle g_{\bar{n}\bar{m}} \langle \bar{m}| \quad (2.11)$$

where the prime indicates a sum over states  $|\bar{n}\rangle, |\bar{m}\rangle$  orthogonal to open channels.

If the lead belonging to channel  $n$  terminates at  $x = x_L$ , then on the surface of the lead, the Green’s function  $g_n(x, x')$  takes the form  $g_n(x_L, x_L) = g_n$ , where  $g_n = a_n - ib_n$ , with  $a_n$  real and  $b_n$  equal to  $\pi$  times the density of states per unit length of channel  $n$ . Furthermore, if  $v_n$  is the group velocity for a wavepacket travelling along channel  $n$ , then  $\hbar v_n = 2b_n/|g_n|^2$ . For example, for a normal lead terminating at  $x = x_L$  and described by a tight-binding Hamiltonian of the form

$$H_{0L} = \sum_{\mathbf{r}} \epsilon_0 |\mathbf{r}\rangle \langle \mathbf{r}| - \sum_{\substack{\mathbf{r}' \\ \text{nearest} \\ \text{neighbours}}} \gamma |\mathbf{r}\rangle \langle \mathbf{r}'|$$

one obtains

$$g_n(x, x') = [1/(\hbar v_n)]\{\exp[ik_x^n|x - x'|] - \exp[-ik_x^n(x + x' - 2(x_L + a))]\}$$

where  $k_x^n$  is the longitudinal wavevector of channel  $n$ . From this expression it is clear that if  $x$  and  $x'$  are positions located between  $x_L$  and some point  $x_n$ , then

$$g_n(x, x_n)g_n^*(x', x_n) = \frac{-2}{\hbar v_n} \text{Im} g_n(x, x') = \frac{-2}{\hbar v_n} \text{Im} g_n(x', x). \quad (2.12)$$

If  $x_n$  is some asymptotic position far from the closed end of the lead containing channel  $n$  and far from the scattering region (i.e. contact) defined by  $H_1$ , then the transmission coefficient from channel  $n'$  to channel  $n$  ( $n \neq n'$ ) is [18, 32]

$$T_{nn'} = \hbar v_n \hbar v_{n'} | \langle n, x_n | G_{AA} | n', x_{n'} \rangle |^2 \quad (2.13)$$

and since

$$\langle n, x_n | G_{AA} | n', x_{n'} \rangle = \sum_{x, x'} g_n(x_n, x) \langle n, x | W G_{BB} W^\dagger | n', x' \rangle g_{n'}(x', x_{n'})$$

one obtains

$$T_{nn'} = 4 \sum_{\substack{x, x' \\ \bar{x}, \bar{x}'}} [\text{Im} g_n(\bar{x}, x)] \langle n, x | W G_{BB} W^\dagger | n', x' \rangle \langle n, \bar{x} | W G_{BB} W^\dagger | n', \bar{x}' \rangle^* [\text{Im} g_{n'}(x', \bar{x}')]. \quad (2.14)$$

To obtain equation (2.3a), we introduce eigenstates of  $H_B$ , satisfying  $H_B |f_\nu\rangle = \epsilon_\nu |f_\nu\rangle$  and write

$$g_B = \sum_\nu \frac{|f_\nu\rangle \langle f_\nu|}{E - \epsilon_\nu}. \quad (2.15)$$

From the expression for  $G_{BB}$  given in equation (2.6), this yields

$$G_{BB} = (g_B^{-1} - W^\dagger g_A W)^{-1} = \sum_{\mu, \nu} |f_\mu\rangle \langle G_{BB} \rangle_{\mu\nu} \langle f_\nu| \quad (2.16)$$

where

$$\langle G_{BB}^{-1} \rangle_{\mu\nu} = (E - \epsilon_\nu) \delta_{\mu\nu} - \langle f_\mu | W^\dagger g_A W | f_\nu \rangle. \quad (2.17)$$

Combining this with equation (2.11) yields

$$\begin{aligned} \langle G_{BB}^{-1} \rangle_{\mu\nu} &= (E - \epsilon_\nu) \delta_{\mu\nu} - \sum_{x, x'} \langle f_\mu | W^\dagger | n, x \rangle g_n(x, x') \langle n, x' | W | f_\nu \rangle \\ &\quad - \sum_{\bar{n}\bar{m}} \langle f_\mu | W^\dagger | \bar{n} \rangle g_{\bar{n}\bar{m}} \langle \bar{m} | W | f_\nu \rangle. \end{aligned} \quad (2.18)$$

In general, since the (on-shell) energy  $E$  lies in a region where the contribution to the density of states from  $g_{\bar{n}\bar{m}}$  is zero,  $\text{Im } g_{\bar{n}\bar{m}} = 0$  and  $g_{\bar{n}\bar{m}} = g_{\bar{n}\bar{m}}^*$ . For this reason it is convenient to introduce the notation

$$\sigma'_{\mu\nu} = \sum_{\bar{n}\bar{m}} \langle f_\mu | W^\dagger | \bar{n} \rangle g_{\bar{n}\bar{m}} \langle \bar{m} | W | f_\nu \rangle \quad (2.19)$$

$$\sigma_{\mu\nu}(n) = \sum_{x,x'} \langle f_\mu | W^\dagger | n, x \rangle [\text{Re } g_n(x, x')] \langle n, x' | W | f_\nu \rangle \quad (2.20)$$

$$\sigma_{\mu\nu} = \sum_n \sigma_{\mu\nu}(n) \quad (2.21)$$

$$\Sigma_{\mu\nu} = \sigma_{\mu\nu} + \sigma'_{\mu\nu} \quad (2.22)$$

$$\Gamma_{\mu\nu}(n) = - \sum_{x,x'} \langle f_\mu | W^\dagger | n, x \rangle [\text{Im } g_n(x, x')] \langle n, x' | W | f_\nu \rangle \quad (2.23)$$

and

$$\Gamma_{\mu\nu} = \sum_n \Gamma_{\mu\nu}(n). \quad (2.24)$$

Clearly the matrices  $\sigma'$ ,  $\sigma(n)$  and  $\Gamma(n)$  are Hermitian. With this notation

$$(G_{BB}^{-1})_{\mu\nu} = (E - \epsilon_\nu) \delta_{\mu\nu} - \Sigma_{\mu\nu} + i\Gamma_{\mu\nu} \quad (2.25)$$

or, alternatively,

$$(G_{BB}^{-1})_{\mu\nu} = (G'^{-1}_{BB})_{\mu\nu} - \sigma_{\mu\nu} + i\Gamma_{\mu\nu} \quad (2.26)$$

where  $G'_{BB}$  is the Green's function arising before open channels of external leads are connected to the dot, given by

$$(G'^{-1}_{BB})_{\mu\nu} = (E - \epsilon_\nu) \delta_{\mu\nu} - \sigma'_{\mu\nu}. \quad (2.27)$$

Furthermore equation (2.14) becomes

$$T_{nn'} = 4 \sum_{\mu\nu\mu'\nu'} \Gamma_{\mu'\mu}(n) (G_{BB})_{\mu\nu} (G_{BB})_{\mu'\nu'}^* \Gamma_{\nu\nu'}(n') \quad (2.28)$$

which completes the derivation of equation (2.3a). The derivation of equation (2.3b) is a straightforward extension of the above analysis, starting from the fundamental relation

$$T_{nn} = (\hbar v_n)^2 |\langle n, x_n | G_{AA} | n, x_n \rangle - 1|^2.$$

### 3. Expressions for scattering coefficients in the presence of Andreev scattering

In this section we collect together some general formulae for use in later sections. Equation (2.3a) or equivalently (2.28) immediately yields expressions for the coefficients  $P_{ij}^{\alpha\beta}(E, H)$  introduced in appendix A. Indeed for  $n \neq n'$ , following the notation of appendix A and writing  $n = (i, a, \alpha)$ ,  $n' = (j, b, \beta)$ , yields

$$P_{ij}^{\alpha\beta}(E, H) = 4 \sum_{\mu\nu\mu'\nu'} \Gamma_{\mu'\mu}(i, \alpha) (G_{BB})_{\mu\nu} (G_{BB})_{\mu'\nu'}^* \Gamma_{\nu\nu'}(j, \beta) \quad (3.1)$$

where

$$\Gamma_{\mu'\mu}(i, \alpha) = \sum_a \Gamma_{\mu'\mu}(i, a, \alpha). \quad (3.2)$$

For structures where transport is dominated by quasi-particle resonances, only those levels with  $\epsilon_\nu \approx E$  are important, and therefore a good approximation is obtained by restricting the sums on the right-hand side of equations (2.15) and (3.1) to a small number of states. The standard Breit-Wigner formula is obtained by keeping only a single term, which yields

$$G_{BB} = \frac{|f_\nu\rangle\langle f_\nu|}{(E - \epsilon_\nu) - \Sigma_{\nu\nu} + i\Gamma_{\nu\nu}} \quad (3.3)$$

and

$$P_{ij}^{\alpha\beta}(E, H) = \frac{4\Gamma_{\nu\nu}(i, \alpha)\Gamma_{\nu\nu}(j, \beta)}{|(E - \epsilon_\nu) - \Sigma_{\nu\nu} + i\Gamma_{\nu\nu}|^2}. \quad (3.4)$$

In situations where the structure  $B$  contains degeneracies, it may be necessary to retain two terms, which we label with indices  $\nu = +$  and  $\nu = -$ . In this case

$$G_{BB}^{-1} = \sum_{\nu, \nu' = \pm} |f_\nu\rangle\langle f_{\nu'}| \quad (3.5)$$

where the  $2 \times 2$  matrix  $\mathbf{G}_{BB}$  is given by

$$\mathbf{G}_{BB}^{-1} = \begin{pmatrix} [E - \epsilon_+ - \Sigma_{++} + i\Gamma_{++}] & [-\Sigma_{+-} + i\Gamma_{+-}] \\ [-\Sigma_{-+} + i\Gamma_{-+}] & [E - \epsilon_- - \Sigma_{--} + i\Gamma_{--}] \end{pmatrix}. \quad (3.6)$$

This yields

$$G_{BB} = \sum_{\nu, \nu' = \pm} |f_\nu\rangle\langle f_{\nu'}| \quad (3.7)$$

where

$$\mathbf{G}_{BB} = \frac{1}{d} \begin{pmatrix} [E - \epsilon_- - \Sigma_{--} + i\Gamma_{--}] & [\Sigma_{+-} - i\Gamma_{+-}] \\ [\Sigma_{-+} - i\Gamma_{-+}] & [E - \epsilon_+ - \Sigma_{++} + i\Gamma_{++}] \end{pmatrix} \quad (3.8)$$

with

$$d = (E - \epsilon_+ - \Sigma_{++} + i\Gamma_{++})(E - \epsilon_- - \Sigma_{--} + i\Gamma_{--}) - (\Sigma_{+-} - i\Gamma_{+-})(\Sigma_{-+} - i\Gamma_{-+}). \quad (3.9)$$

For situations in which the coupling matrix  $W$  between the dot and leads is diagonal in quasi-particle indices, we write

$$W = \begin{pmatrix} W^+ & 0 \\ 0 & W^- \end{pmatrix} \quad (3.10)$$

and

$$|f_\nu\rangle = \begin{pmatrix} |f_\nu^+\rangle \\ |f_\nu^-\rangle \end{pmatrix} \quad (3.11)$$

where  $W^- = -(W^+)^*$ . Furthermore for certain structures, such as those considered in sections 5 and 6,  $|f_\nu^\pm\rangle$  are related by

$$|f_\nu^\alpha\rangle = u_\nu^\alpha |\phi_\alpha\rangle. \quad (3.12)$$

In this case one obtains

$$\Gamma_{\mu\nu} = \sum_\alpha (u_\mu^\alpha)^* u_\nu^\alpha \Gamma_\alpha \quad (3.13)$$

$$\sigma_{\mu\nu} = \sum_\alpha (u_\mu^\alpha)^* u_\nu^\alpha \sigma_\alpha \quad (3.14)$$

and

$$\sigma'_{\mu\nu} = \sum_{\alpha,\beta} (u_\mu^\alpha)^* u_\nu^\beta \bar{\sigma}'_{\alpha\beta} \quad (3.15)$$

where

$$\Gamma_\alpha = \sum_i \Gamma(i, \alpha) \quad (3.16)$$

$$\sigma_\alpha = \sum_i \sigma(i, \alpha) \quad (3.17)$$

$$\bar{\sigma}'_{\alpha\beta} = \sum_{\bar{n}, \bar{m}} \sigma'(\bar{n}\alpha, \bar{m}\beta) \quad (3.18)$$

with

$$\Gamma(i, \alpha) = - \sum_{a,x,x'} \langle \phi_\alpha | W^\dagger | i, a, \alpha, x \rangle [\text{Im } g_n(x, x')] \langle i, a, \alpha, x' | W | \phi_\alpha \rangle \quad (3.19)$$

$$\sigma(i, \alpha) = \sum_{a,x,x'} \langle \phi_\alpha | W^\dagger | i, a, \alpha, x \rangle [\text{Re } g_n(x, x')] \langle i, a, \alpha, x' | W | \phi_\alpha \rangle \quad (3.20)$$

and

$$\sigma'(\bar{n}\alpha, \bar{m}\beta) = \sum_a \langle \phi_\alpha | W^{\alpha\dagger} | \bar{n} \rangle g_{\bar{n}\bar{m}} \langle \bar{m} | W^\beta | \phi_\beta \rangle. \quad (3.21)$$

These formulae are valid in the presence of an arbitrary number of leads and illustrate the dependence of transport properties on the coherence factors  $u_\mu^\alpha$ .

#### 4. The Breit–Wigner formula for a N–SDOT–N structure

In this section we consider a superconducting dot with a uniform order parameter, connected to two normal leads. The eigenstates of a superconducting dot satisfy

$$H_B|f_\nu\rangle = \epsilon_\nu|f_\nu\rangle \quad (4.1)$$

where  $H_B$  is the Bogoliubov–de Gennes operator for the isolated dot. If  $|\phi\rangle$  is an eigenstate of the normal dot satisfying  $H_0|\phi\rangle = \epsilon_\nu^0|\phi\rangle$ , then for a dot with a uniform real order parameter  $\Delta_0$ , the solutions of equation (4.1) are of the form

$$\epsilon_\nu = \sqrt{(\epsilon_\nu^0)^2 + \Delta_0^2} \quad (4.2)$$

$$|f_\nu\rangle = \begin{pmatrix} |f_\nu^+\rangle \\ |f_\nu^-\rangle \end{pmatrix} = \begin{pmatrix} u_\nu^+|\phi\rangle \\ u_\nu^-|\phi\rangle \end{pmatrix} \quad (4.3)$$

where

$$u_\nu^+ = \sqrt{\frac{1}{2} \left( 1 + \frac{\epsilon_\nu^0}{\epsilon_\nu} \right)} \quad u_\nu^- = \sqrt{\frac{1}{2} \left( 1 - \frac{\epsilon_\nu^0}{\epsilon_\nu} \right)}. \quad (4.4)$$

Hence the notation of equations (3.12) to (3.21) can be used, and within a single-level approximation, provided either  $i \neq j$  or  $\alpha \neq \beta$ , equations (3.4) and (3.13)–(3.15) yield

$$P_{ij}^{\alpha\beta}(E, H) = 4|u_\nu^\alpha|^2|u_\nu^\beta|^2\Gamma(i, \alpha)\Gamma(j, \beta) / \left( \left| (E - \epsilon_\nu) - \sum_\alpha |u_\nu^\alpha|^2\Sigma_\alpha + i \sum_\alpha |u_\nu^\alpha|^2\Gamma_\alpha \right|^2 \right) \quad (4.5)$$

where  $\Sigma_\alpha = \sigma_\alpha + \sigma'_\alpha$ . The remaining four coefficients are obtained via equation (A1), which yields

$$P_{11}^{++}(E, H) = N_1^+(E) - P_{11}^{-+}(E, H) - P_{21}^{++}(E, H) - P_{21}^{-+}(E, H) \quad (4.6)$$

$$P_{22}^{++}(E, H) = N_2^+(E) - P_{22}^{-+}(E, H) - P_{12}^{++}(E, H) - P_{12}^{-+}(E, H) \quad (4.7)$$

$$P_{11}^{--}(E, H) = N_1^-(E) - P_{11}^{+-}(E, H) - P_{21}^{--}(E, H) - P_{21}^{+-}(E, H) \quad (4.8)$$

$$P_{22}^{--}(E, H) = N_2^-(E) - P_{22}^{+-}(E, H) - P_{12}^{--}(E, H) - P_{12}^{+-}(E, H). \quad (4.9)$$

These coefficients can be used to calculate the matrix elements  $a_{ij}$  of equation (A6) and hence the various response coefficients discussed in appendix A. As an example, we now consider the change in conductance of the dot, due to the switching on of superconductivity. This problem is motivated by recent studies [27–30], which show that when superconductivity is induced in a normal conductor, there are three scenarios for the resulting change in conductance. If the normal-state conductance is high enough, a theorem by Lambert and Hui [27, 28] states that the conductance must *decrease* and

for weakly disordered samples may either decrease or increase depending on the precise impurity configuration. On the other hand for diffusive normal conductors, the conductance typically increases. The third scenario arises in strongly disordered conductors, where it is again found that the conductance may either increase or decrease, depending on the precise realization of the impurity potential. It has been suggested [27] that this behaviour arises through the presence of normal-state, resonant transport and therefore should be contained in equation (4.5).

To investigate this possibility, we consider, for simplicity, the zero-energy limit, where the particle-hole symmetry relation  $P_{ij}^{\alpha\beta}(0, H) = P_{ij}^{-\alpha-\beta}(0, H)$  can be used to simplify the above expressions. In this limit we write  $\Gamma_i = \Gamma(i, \alpha) = \Gamma(i, -\alpha)$  and  $\Sigma = \Sigma_- = -\Sigma_+ > 0$ . Then adopting the notation of equation (A12), one obtains

$$R_a = \frac{4|u_v^+|^2|u_v^-|^2\Gamma_1^2}{|- \epsilon_v + \Sigma\epsilon_v^0/\epsilon_v + i(\Gamma_1 + \Gamma_2)|^2} \quad (4.10)$$

$$R'_a = \frac{4|u_v^+|^2|u_v^-|^2\Gamma_2^2}{|- \epsilon_v + \Sigma\epsilon_v^0/\epsilon_v + i(\Gamma_1 + \Gamma_2)|^2} \quad (4.11)$$

$$T_0 = T'_0 = \frac{4|u_v^+|^4\Gamma_1\Gamma_2}{|- \epsilon_v + \Sigma\epsilon_v^0/\epsilon_v + i(\Gamma_1 + \Gamma_2)|^2} \quad (4.12)$$

$$T_a = T'_a = \frac{4|u_v^+|^2|u_v^-|^2\Gamma_1\Gamma_2}{|- \epsilon_v + \Sigma\epsilon_v^0/\epsilon_v + i(\Gamma_1 + \Gamma_2)|^2}. \quad (4.13)$$

Substituting these coefficients into equation (A12) yields for the zero-voltage conductance

$$G = \frac{4|u_v^+|^2\Gamma_1\Gamma_2}{|- \epsilon_v + \Sigma\epsilon_v^0/\epsilon_v + i(\Gamma_1 + \Gamma_2)|^2}. \quad (4.14)$$

If  $\delta\epsilon$  is the level spacing of the normal-state dot, then equation (4.14) reveals that if  $|\Delta_0| > \delta\epsilon \gg (\Gamma_1 + \Gamma_2)$  then the contribution to the conductance from a single level is of order

$$G = \frac{2\Gamma_1\Gamma_2}{|\Delta_0|^2} \ll 1. \quad (4.15)$$

Similarly, the contribution from all levels is obtained by integrating over  $\epsilon_v$  to yield  $G \approx 2\Gamma_1\Gamma_2/(\delta\epsilon|\Delta_0|)$ . Hence for a large enough value of  $\Delta_0/\Gamma_i$ , all resonances will be suppressed. This result is not unexpected, since in this limit, all transmission coefficients are small and the resistance reduces to the sum of two BTK boundary resistances. If the normal-state system is on-resonance, then switching on superconductivity will decrease  $G$ . This behaviour is typical of a N-S tunnel junction and can be quantified by introducing the  $\Delta$  susceptibility [27, 28]  $\chi_\Delta = \lim_{|\Delta| \rightarrow 0} (\partial G / \partial |\Delta|^2)$ , obtained by differentiating equation (4.15):

$$\begin{aligned} \chi_\Delta &= \lim_{|\Delta| \rightarrow 0} \left( \frac{\partial G}{\partial \epsilon_v} \frac{\partial \epsilon_v}{\partial |\Delta|^2} \right) = \frac{1}{2\epsilon_v^0} \lim_{|\Delta| \rightarrow 0} \frac{\partial G}{\partial \epsilon_v} \\ &= -\frac{\Gamma_1\Gamma_2}{(\epsilon_v^0)^2} \left( \frac{1}{(\epsilon_v^0 - \Sigma)^2 + (\Gamma_1 + \Gamma_2)^2} + \frac{4((\epsilon_v^0)^2 - \Sigma^2)}{((\epsilon_v^0 - \Sigma)^2 + (\Gamma_1 + \Gamma_2)^2)^2} \right). \quad (4.16) \end{aligned}$$

This result demonstrates that although  $\chi_\Delta$  is typically negative, anomalous positive values can arise when  $\Sigma > \epsilon_v^0$ . Since  $\epsilon_v^0$  will be randomly spread between  $-\delta\epsilon/2$  and  $\delta\epsilon/2$  this suggests that the probability,  $P_{+ve}$ , of finding a positive  $\chi_\Delta$  is approximately  $\Sigma/\delta\epsilon$ . For a tight-binding model, in which the coupling matrix  $W^+$  of equation (3.10) is characterized by a coupling constant  $v$ , one finds  $\Sigma \sim N(0)v^2$ , where  $N(0)$  is of order the density of states per site in the normal leads and therefore we expect  $P_{+ve}$  to be proportional to  $(N(0)v^2/\delta\epsilon)$ . Thus the sign of  $\chi_\Delta$  is indeed determined by the presence of normal-state resonances.

### 5. The Breit–Wigner formula for a structure composed of a normal lead, normal dot and a superconducting lead

In this section, we consider a normal dot in contact with several normal leads and one or more superconductors. At zero energy, if the isolated normal dot is on-resonance, then particle–hole symmetry ensures that a degeneracy occurs. Hence in this example the two-level formula (3.8) for  $G_{BB}$  must be employed.

There are two equivalent strategies for tackling this problem. On the one hand one could identify the normal dot with sub-space  $B$  of section 2 and associate the superconducting and normal leads with sub-space  $A$ . In this case, for energies less than the energy gap, the superconducting contact contributes only to the self-energy  $\sigma'$ . On the other hand, one could identify the normal dot plus superconductor(s) with the sub-space  $B$  and the single normal lead with sub-space  $A$ .

In what follows we adopt the former approach and for simplicity consider energies at which there are no open channels in the superconductor(s). It can be shown that at the end of a superconducting lead with a uniform order parameter  $\Delta_L = |\Delta_L|e^{i\phi_L}$ , the causal Green's function can be written as

$$g_L^{\sigma\sigma'}(x_L, y, x_L, y', E) = \sum_{n=1}^M \chi_n(y)\chi_n(y')g_L^{\sigma\sigma'}(x_L, x_L, n, E)$$

where  $g_L^{\sigma\sigma'}(x_L, x_L, n, E)$  has the structure

$$\begin{pmatrix} g_L^{++}(x_L, x_L, n, E) & g_L^{+-}(x_L, x_L, n, E) \\ g_L^{-+}(x_L, x_L, n, E) & g_L^{--}(x_L, x_L, n, E) \end{pmatrix} = \begin{pmatrix} A_n & B_n e^{i\phi_L} \\ B_n e^{-i\phi_L} & C_n \end{pmatrix}.$$

For energies below the gap,  $A_n, B_n, C_n$  are real, while for energies above the gap they are complex. Hence for energies below the gap, equation (3.8) takes the form

$$G_{BB} = \frac{1}{d} \begin{pmatrix} E - \epsilon_- - \Sigma_{--} + i\Gamma_- & \sigma'_{+-} \\ \sigma'_{-+} & E - \epsilon_+ - \Sigma_{++} + i\Gamma_+ \end{pmatrix} \quad (5.1)$$

where

$$d = (E - \epsilon_+ - \Sigma_{++} + i\Gamma_+)(E - \epsilon_- - \Sigma_{--} + i\Gamma_-) - |\sigma'_{+-}|^2. \quad (5.2)$$

In the presence of a single normal lead, we focus on the Andreev reflection coefficient  $P_{11}^{-+}(E, H)$ , and since the coherence factors of equation (3.12) take the form  $u_v^\alpha = \delta_{\alpha v}$ , the electrical conductance (2.9) reduces to

$$G = 2P_{11}^{-+}(E, H) = \frac{8\Gamma_+\Gamma_-|\sigma'_{+-}|^2}{|d|^2} \quad (5.3)$$

First consider the zero-energy limit, where particle-hole symmetry implies that the two levels closest to  $E = 0$  satisfy  $\epsilon_- = -\epsilon_+$  and therefore a vanishing particle level  $\epsilon_+$  is accompanied by a degeneracy. In this limit,  $\Sigma_{--} = -\Sigma_{++}$  and  $\Gamma_- = \Gamma_+$ . Hence

$$G = \frac{8\Gamma_+^2\sigma'_{+-}\sigma'_{-+}}{((\epsilon_+ + \Sigma_{++})^2 + \Gamma_+^2 + |\sigma'_{+-}|^2)^2} \tag{5.4}$$

which was obtained in [10] for resonant transport at zero energy. It is interesting to compare the probability of finding a resonance in such a N-NDOT-S structure with the corresponding probability (equation (1.1)) of the N-NDOT-N structure arising when the superconducting order parameter is allowed to vanish. If  $|\sigma'_{+-}|^2 = \Gamma_+^2$ , then a resonance will occur when  $\epsilon_+ + \Sigma_{++} = 0$ . Since this involves only a single condition on the  $\epsilon_+$ , one expects resonances to occur with approximately the same probability in the two structures.

However, at finite energies, equation (5.2) reveals that this result is drastically modified, because a resonance can now occur only if both  $(E - \epsilon_+ - \Sigma_{++} = 0)$  and  $(E - \epsilon_- - \Sigma_{--} = 0)$ . The probability of simultaneously satisfying both of these conditions is small and therefore we predict that the breaking of the particle-hole symmetry at  $E \neq 0$  destroys finite-voltage conductance resonances.

To quantify this behaviour, we now examine the denominator  $D = |d|^2$  of equation (5.3), which can be written as

$$D = |(E - \lambda_+)(E - \lambda_-) + i[\Gamma_+(E - \epsilon_- - \Sigma_{--}) + \Gamma_-(E - \epsilon_+ - \Sigma_{++})]|^2 \\ = ((E - \lambda_+)(E - \lambda_-))^2 + (\Gamma_+ + \Gamma_-)^2(E - \theta)^2 \tag{5.5}$$

where

$$\lambda_{\pm} = \frac{(\epsilon_+ + \Sigma_{++}) + (\epsilon_- + \Sigma_{--})}{2} \\ \pm \sqrt{\left(\frac{(\epsilon_+ + \Sigma_{++}) - (\epsilon_- + \Sigma_{--})}{2}\right)^2 + \sigma'_{+-}\sigma'_{-+} + \Gamma_+\Gamma_-} \\ = \Xi \pm R \tag{5.6}$$

and

$$\theta = \frac{(\epsilon_+ + \Sigma_{++}) + (\epsilon_- + \Sigma_{--})}{2} + \frac{((\epsilon_+ + \Sigma_{++}) - (\epsilon_- + \Sigma_{--}))(\Gamma_+ - \Gamma_-)}{2(\Gamma_- + \Gamma_+)} = \Xi + \delta. \tag{5.7}$$

In the limit where the strength of the contact to the normal lead vanishes (i.e. when  $\Gamma_{\alpha} = 0$ ),  $\lambda_{\pm}$  reduces to the eigenenergies of the isolated NDOT-S composite. This demonstrates that when contact is made between the NDOT and the superconductor there is a splitting of the energy levels of the normal dot due to the proximity of the superconducting lead, but no broadening of the levels.

Writing  $\eta = E - \Xi$  and  $\rho = (\Gamma_+ + \Gamma_-)^2$  yields

$$D = (\eta^2 - R^2)^2 + \rho(\eta - \delta)^2. \tag{5.8}$$

If the energy  $E$  is varied, then the resonance condition becomes

$$\frac{\partial D}{\partial \eta} = 4\eta^3 + (2\rho - 4R^2)\eta - 2\rho\delta = 0 \tag{5.9}$$

which has one solution if  $(2\rho - 4R^2) \geq 0$ , but the possibility of three solutions if  $(2\rho - 4R^2) < 0$ . To obtain three solutions, there must be two turning points, which occur at  $\eta = \pm\sqrt{(R^2 - \rho/2)/3}$ . Hence we predict that a double resonance can occur when

$$\left| \frac{\rho\delta}{2} \right| < \frac{2(R^2 - \rho/2)^{3/2}}{3\sqrt{3}} \quad \text{and} \quad 2\rho - 4R^2 < 0. \quad (5.10)$$

To illustrate the structure of these resonances, figure 2 shows plots of  $P_{11}^{-+}(E, H)$ , obtained from equation (5.3), for various values of coupling to the normal lead; figure 2(a) has the strongest coupling and 2(d) the weakest. All quantities are plotted as functions of quasi-particle energy  $E$ , which is a measure of the parameter  $\eta$ . Hence as well as a drastic reduction in the probability of finding finite-energy resonances, we predict that in the weak-coupling limit, when a resonance does occur, the usual Lorentzian line-shape is replaced by a double-peaked structure, with different peak heights determined by the difference between  $\Gamma_+$  and  $\Gamma_-$  at finite energies.

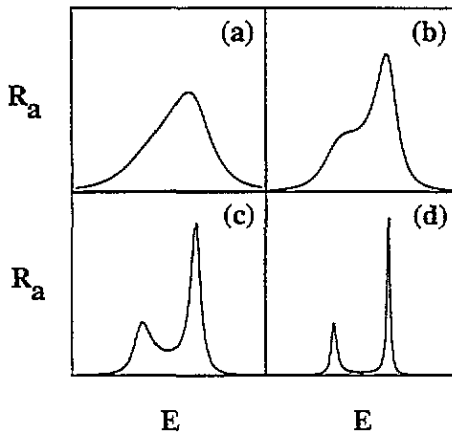


Figure 2. (a) to (d) show plots of equation (5.3) against energy  $E$ , for decreasing values of the coupling to the normal lead.

## 6. Analysis of resonant SEQUINs

When a composite N-SS' or N-NDOT-SS' structure is formed from two or more superconductors, with different order parameter phases, or from a single superconductor with an imposed phase gradient [46], transport properties can be significantly modified if the phase difference between two points is varied by  $2\pi$  [15–22]. In experimental realizations of such SEQUINs [23–26], the phase difference between two superconducting contacts is modulated by connecting the superconductors to a macroscopic, external superconducting loop, whose phase is controlled by an applied magnetic field. Sub-gap quasi-particles can penetrate only a distance of order the superconducting coherence length into the superconductor and therefore apart from controlling the phase, the macroscopic loop plays no role in determining the  $s$ -matrix of the region near the contacts. Since the electrical conductance is a periodic function of the phase difference  $\eta$ , with period  $2\pi$ , and since  $\eta$  changes by  $2\pi$  when the flux  $\Phi$  through the macroscopic control-loop changes by a flux quantum  $\Phi_0$ , a SEQUIN is a galvanometric detector of flux, with a sensitivity comparable

with that of a SQUID. In this section we highlight generic properties of resonant SEQUINs and predict that flux sensitivity is significantly enhanced by the presence of resonances.

The starting point for this analysis is a sub-space  $B$  containing one or more superconductors, with eigenstates  $|f_\nu\rangle$  and eigenvalues  $\epsilon_\nu$ , which are periodic functions of some dimensionless parameter  $\eta$ , with period  $2\pi$ . Before attaching the normal lead, the Green's function of such a structure is given by equation (2.15) and for a sub-gap energy  $E$ , when contact is made with the normal lead, equations (3.4) and (A9) yield for the BTK conductance

$$G(\eta) = \frac{8\Gamma_\nu(\eta, +)\Gamma_\nu(\eta, -)}{|(E - \epsilon_\nu(\eta)) - \Sigma_\nu(\eta) + i\Gamma_\nu(\eta)|^2}. \quad (6.1)$$

For a coupling matrix of the form (3.10) and eigenstates of the form (3.11), one obtains

$$\Gamma_\nu(\eta) = \sum_\alpha \Gamma_\nu(\eta, \alpha) \quad (6.2)$$

$$\Sigma_\nu(\eta) = \sum_\alpha \sigma_\nu(\eta, \alpha) \quad (6.3)$$

where

$$\Gamma_\nu(\eta, \alpha) = - \sum_{a,x,x'} \langle f_\nu^\alpha | W^\dagger | 1, a, \alpha, x \rangle [\text{Im } g_n(x, x')] \langle 1, a, \alpha, x' | W | f_\nu^\alpha \rangle \quad (6.4)$$

and

$$\Sigma_\nu(\eta, \alpha) = \sum_{a,x,x'} \langle f_\nu^\alpha | W^\dagger | 1, a, \alpha, x \rangle [\text{Re } g_n(x, x')] \langle 1, a, \alpha, x' | W | f_\nu^\alpha \rangle. \quad (6.5)$$

Consider now the situation in which, at  $\eta = \eta_0$ , the resonance condition  $E - \bar{\Sigma}_\nu(\eta_0) = 0$  is satisfied, where  $\bar{\Sigma}_\nu(\eta) = \epsilon_\nu(\eta) + \Sigma_\nu(\eta)$ . Then expanding equation (6.1) about  $\eta_0$  yields

$$G(\eta) = \frac{8\Gamma_\nu(\eta_0, +)\Gamma_\nu(\eta_0, -)}{[\partial \bar{\Sigma}_\nu(\eta_0)/\partial \eta_0]^2 [\eta - \eta_0]^2 + \Gamma_\nu^2(\eta_0)}. \quad (6.6)$$

This demonstrates that with varying  $\eta$ ,  $G$  exhibits a Lorentzian resonance of width  $\Gamma_\nu(\eta_0)/[\partial \bar{\Sigma}_\nu(\eta_0)/\partial \eta_0]$ .

For the case  $\eta = 2\pi\Phi/\Phi_0$ , noting that  $\bar{\Sigma}_\nu(\eta)$  can vary by at most an amount of order  $\Delta_0$  as  $\eta$  varies by  $2\pi$  yields an upper bound for  $[\partial \bar{\Sigma}_\nu(\eta_0)/\partial \eta_0]$  of order  $\Delta_0/2\pi$ . Hence in terms of the flux through the external control loop, the resonance width is greater than or of the order of

$$\delta\Phi = 2\pi\Phi_0\Gamma_\nu(\eta_0)/\Delta_0. \quad (6.7)$$

For simplicity in the above analysis, we have considered only a single resonance and a normal lead with no closed channels; the latter merely shifts the position of the resonance, while the former may lead to the appearance of several resonances per flux quantum. If the temperature  $T$  is greater than  $\Gamma_\nu(\eta_0)/k_B$ , then the resonance width will be of order

$$\delta\Phi = 2\pi\Phi_0k_B T/\Delta_0. \quad (6.8)$$

For a SEQUIN operating at 1 K, formed from a cuprate superconductor with a transition temperature of 100 K, this yields  $\delta\Phi \simeq \Phi_0/20$ .

## 7. Numerical results in two dimensions

In this section, we present the results of detailed numerical simulations of two-dimensional tight-binding systems, described by a tight-binding Bogoliubov–de Gennes operator of the form

$$H \begin{pmatrix} \psi \\ \phi \end{pmatrix} = \begin{pmatrix} H_0 & \Delta \\ \Delta^\dagger & -H_0^* \end{pmatrix} \begin{pmatrix} \psi \\ \phi \end{pmatrix} = E \begin{pmatrix} \psi \\ \phi \end{pmatrix} \quad (7.1)$$

where  $H_0$  is a nearest-neighbour Anderson Hamiltonian on a square lattice with off-diagonal hopping elements of value  $-1$ , and  $\Delta$  is a diagonal matrix. The scattering region is chosen to be  $M$  sites wide and is connected to external leads of width  $M$ . Within a disordered scattering region, diagonal elements  $\{\epsilon_i\}$  of  $H_0$  are chosen to be random numbers, uniformly distributed between  $\epsilon_0 - W$  and  $\epsilon_0 + W$ . Within a superconducting region, those of  $\Delta$  are set equal to  $\Delta_0$ . Within the normal leads, the diagonal elements of  $H_0$  are equal to a constant  $\epsilon_0$ , while those of  $\Delta$  are set to zero. In what follows, for a given realization of the Hamiltonian  $H$ , the scattering matrix is obtained numerically using a transfer matrix technique outlined in appendix 2 of [32].

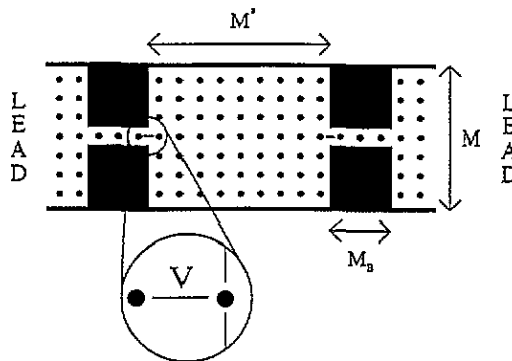
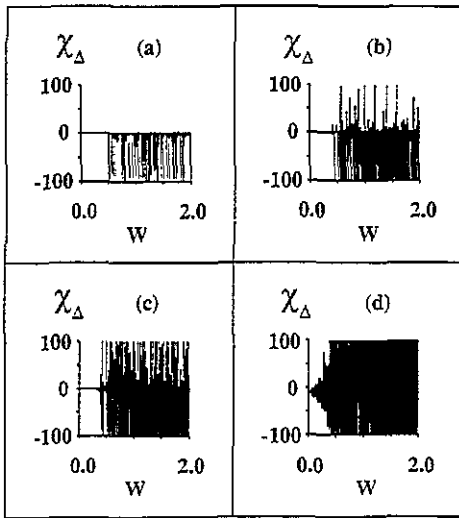


Figure 3. The tight-binding two-dimensional structure used for the N–SDOT–N calculations of figures 4 to 7. The shaded regions denote large insulating regions with diagonal elements  $\epsilon = 100$ . The leads are coupled by a single hopping element of value  $-v$  to one site on the surface of the dot. All other hopping elements are of value  $-1$ . The dot is disordered, with disorder width  $2W$ , and can be either superconducting or normal.

First we present results for the N–SDOT–N structure shown in figure 3, which we compare with the analytic results of section 4. The shaded region in figure 3 denotes a large insulating barrier, obtained by choosing a suitably large value for the diagonal elements of  $H_0$  such that an unbroken barrier of this width would yield no quasi-particle transmission. The system is  $M' + 2M_B$  sites long and the leads are connected to the dot by a one-dimensional channel of length  $M_B$ . A point contact between the channel and dot is made via a hopping element  $-v$ .

For  $E = 0$ , figure 4 shows plots of the  $\Delta$  susceptibility versus the disorder  $W$ , for four coupling strengths  $v$  ranging from  $1/100$  to  $1$ . For the structure used in these calculations,  $\epsilon_0 = 0.2$ ,  $M = 11$ ,  $M' = 10$ ,  $M_B = 5$  and the barriers are identical. Within the barriers, the diagonal element is set to  $100$ . Figure 5 demonstrates that the number of positive values of  $\chi_\Delta$  increases as the strength  $v$  of the contact is increased. To quantify the rate of increase,



**Figure 4.** (a) to (d) show plots of  $\chi_{\Delta}$  against disorder  $W$  for  $v = 0.01, 0.1, 0.2$  and  $1$  respectively with  $M = 11$ ,  $M' = 10$  and  $M_B = 5$ . The vertical scale has been chosen to show typical values of  $\chi_{\Delta}$ . A small number of points, whose values are of order  $-10^6$  to  $-10^8$ , fall outside the vertical range of the plots.

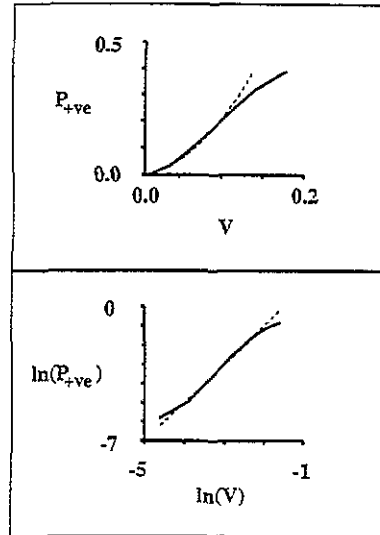


**Figure 5.** The upper panel shows a plot of the probability of finding a positive  $\chi_{\Delta}$  as a function of  $v$ . Superimposed on this is a graph of  $P_{+ve} = Av^2$  (dashed curve) for a choice of the constant  $A$  which yields a best fit. The solid line of the lower panel shows a log-log plot of the numerical results of the upper panel, while the dashed line shows a plot of  $\ln(P_{+ve}) = \ln(A) + 2 \ln(v)$ .

the upper graph of figure 5 shows the probability  $P_{+ve}$  of finding a positive  $\chi_{\Delta}$ , plotted against  $v$ . Superimposed on this curve is a plot of the prediction based on equation (4.16);  $P_{+ve} = A(v)^2$  (dashed line), where  $A$  is a constant. The lower graph of figure 5 shows a plot of  $\ln(P_{+ve})$  versus  $\ln(v)$ , along with the straight (dashed) line  $\ln(P_{+ve}) = \ln(A) + 2 \ln(v)$ , confirming that  $P_{+ve}$  is indeed parabolic for small  $v$ .

As well as the susceptibility  $\chi_{\Delta}$ , it is also of interest to examine the change in conductance  $\delta G$  at finite  $\Delta$ . Figure 6 shows results for the variation of  $\delta G$  with  $\Delta_0$ , for various values of disorder ranging from  $W = 1$  to  $W = 2$ . The model parameter values for this system were  $\epsilon_0 = 0.2$ ,  $M = 11$ ,  $M' = 30$ ,  $M_B = 5$  and  $v = 0.1$ . Figure 6 demonstrates that for systems in which a large variation in the conductance occurs, the change  $\delta G$  is typically negative. For a dot with  $M = 11$ ,  $M' = 10$  and  $M_B = 5$ , figure 7 shows results for the change in conductance due to the switching on of an order parameter of magnitude  $\Delta_0 = 0.01$ , plotted against disorder strength  $W$ , for four values of  $v$  ranging from  $v = 0.01$  to  $v = 1$ . Again for small couplings  $v$ , large negative changes occur when the switching on of  $\Delta_0$  moves the system away from a normal-state resonance. For larger values of  $v$ , not described by the weak-coupling analysis of section 5, figure 7(d) shows that large changes of arbitrary sign can occur.

We now present results for the N-NDOT-S structure shown in figure 8, which we compare with the analytic predictions of section 5. In this figure, the dot is  $M$  sites wide and  $M'$  sites long. The connection to the left-hand lead is  $M_L$  sites wide and via hopping elements  $v_L$ . The right-hand side of the dot is connected via hopping elements  $v_R$  to  $M_R$  sites of a superconducting region. Results for the N-NDOT-N system are obtained by setting  $\Delta_0 = 0$  in the superconducting region and evaluating the conductance using

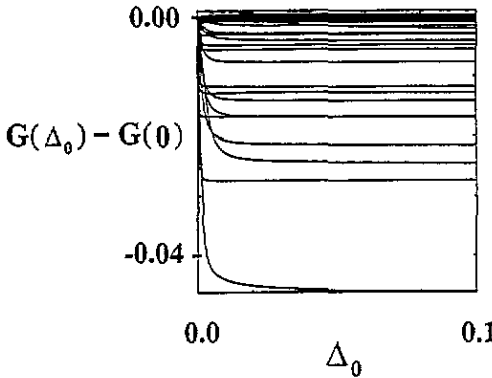


Figure 6. The change in conductance  $\delta G = G(\Delta_0) - G(0)$  against  $\Delta_0$  for 500 realizations of disorder with  $W$  varied from 1 to 2.

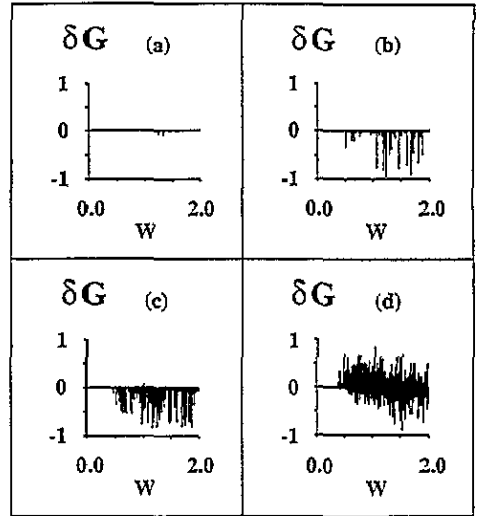


Figure 7. (a) to (d) show the change  $\delta G$  obtained by switching on an order parameter of magnitude  $\Delta_0 = 0.01$ , plotted against  $W$  for  $\nu = 0.01, 0.1, 0.2$  and 1 respectively.

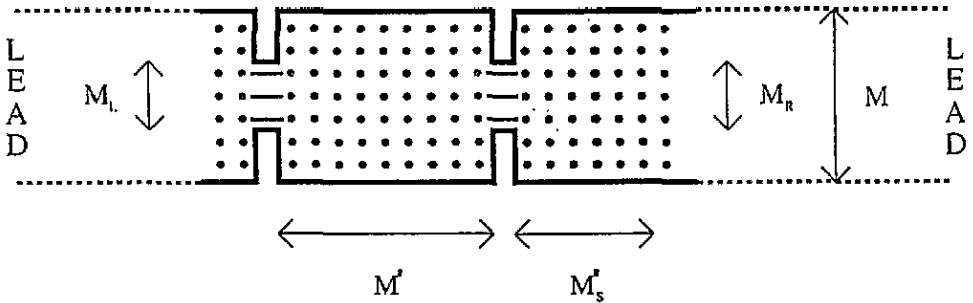


Figure 8. The tight-binding two-dimensional structure used for the N-NDOT-S calculations of figures 9 to 11. The region of length  $M'_S$  denotes a superconducting region of length  $M'_S$  sites with on-site order parameter  $\Delta_0$ , where  $\Delta_0$  and  $M'_S$  were chosen to give zero quasi-particle transmission. The superconductor is coupled to  $M_R$  sites on the surface of the dot, by hopping elements  $\nu_R$ . The left-hand lead is attached to  $M_L$  sites on the dot by hopping elements  $\nu_L$ . The dot is disordered, with disorder width  $2W$ .

the formula  $G = T_0(E)$ . For the N-NDOT-S system,  $\Delta_0$  is set to a finite value and the BTK conductance  $G = 2R_a(E)$  of equation (A9) is evaluated. To ensure negligible transmission through the superconductor, the length  $M'_S$  of the superconductor is chosen such that  $M'_S \gg \xi$ , where  $\xi = 1/\Delta_0$  is the superconducting coherence length. Figures 9 and 10 illustrate the destruction of finite-energy resonances due to the switching on of superconductivity in the right-hand lead. For  $\Delta_0 = 0$ , the upper curves in each figure show results for the normal-state transmission coefficient  $T_0(E)$  as a function of the mean diagonal element  $\epsilon_0$  of  $H_0$ . For  $\Delta_0 \neq 0$ , the lower curves in each figure show the corresponding Andreev reflection coefficient  $R_a(E)$ . Figure 9 shows results for  $E = 0$  and figure 10 for  $E = 0.1$ . In each figure,  $\epsilon_0$  varies over the complete tight-binding energy band, from  $-4$

to  $+4$ . These results were obtained with model parameters  $M = 11$ ,  $M' = 20$ ,  $M'_S = 10$  and  $M_L = M_R = 1$ , with  $v_L = v_R = 0.2$  and  $W = 1.5$ . These results are typical of those obtained for a variety of model parameters, provided the level broadening is smaller than the level spacing of the dot. For the system in which  $\Delta_0$  is finite, a value of  $\Delta_0 = 2$  was used. This value was chosen so that the relatively small dot used in the simulations would possess many quasi-particle levels below the energy gap of the superconductor.

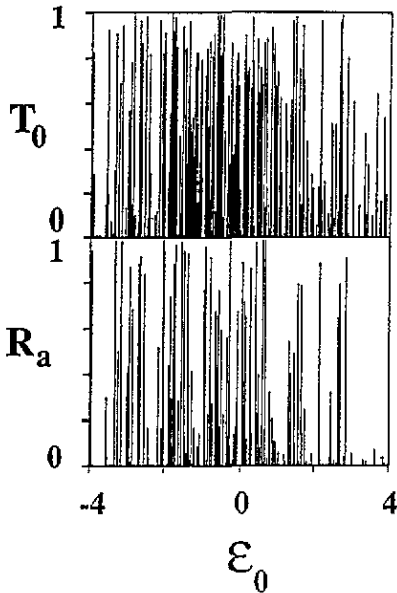


Figure 9. For a quasi-particle energy  $E = 0$ , the top graph shows the transmission coefficient  $T_0$  when  $\Delta_0 = 0$ , as a function of the mean diagonal element  $\epsilon_0$  for the dot. The lower graph shows corresponding results for Andreev reflection coefficient  $R_a$ , when the order parameter in the right-hand lead assumes a non-zero value  $\Delta_0 = 2$ .

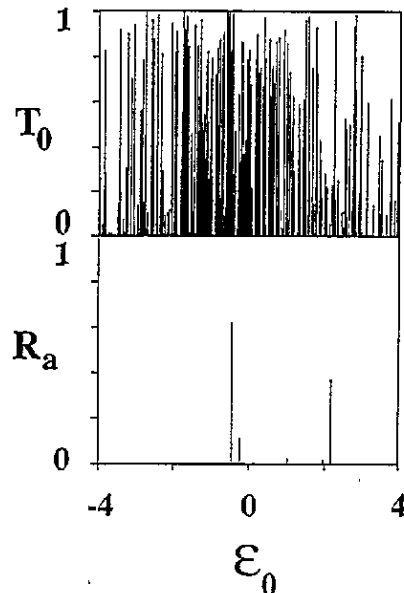


Figure 10. As figure 9, except that the energy now takes the non-zero value  $E = 0.1$ .

As predicted by the analysis of section 6, figure 9 demonstrates that at zero energy, the probability of finding a resonance in the N-NDOT-S structure is slightly smaller than, but of the same order of magnitude as the corresponding probability in the N-NDOT-S system. In contrast at finite energies, figure 10 demonstrates that whereas normal-state transmission resonances survive, resonances in the N-NDOT-S system are almost completely suppressed. Furthermore when a finite-energy resonance in  $R_a(E)$  does occur, the shape of the resonance is no longer Lorentzian. Figures 11(a) to 11(f) show numerical results for a typical resonance belonging a disordered dot with  $W = 0.5$ , for different strengths of coupling to the normal lead; figure 11(a) has the strongest coupling with  $v_L = 0.7$  and 11(f) the weakest coupling with  $v_L = 0.1$ . In each case the coupling to the superconductor was fixed at  $v_R = 0.6$ . These results mirror the analytic results of figure 2 and confirm that finite-energy resonances in  $R_a$  exhibit the expected double-peaked structure.

As a final example, we now show results for the resonant N-SS' structure sketched in figure 12, which comprises a thin superconductor S, separated from a second longer superconductor S' by a normal 2DEG N'. For convenience the superconductor S' is chosen

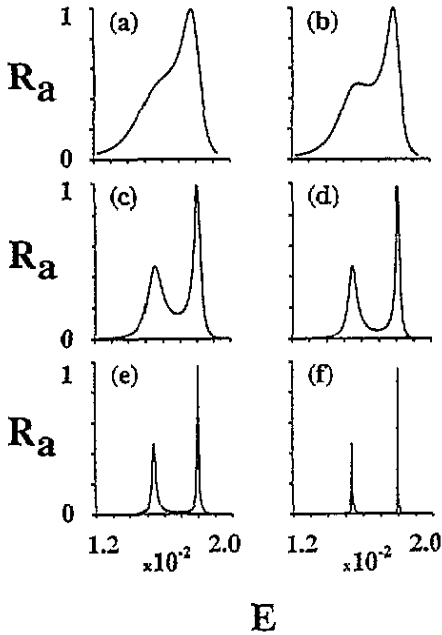


Figure 11. (a) to (f) show numerical results for the Andreev reflection coefficient as a function of  $E$  for  $v_L = 0.7, 0.6, 0.4, 0.3, 0.2$  and  $0.1$  respectively.

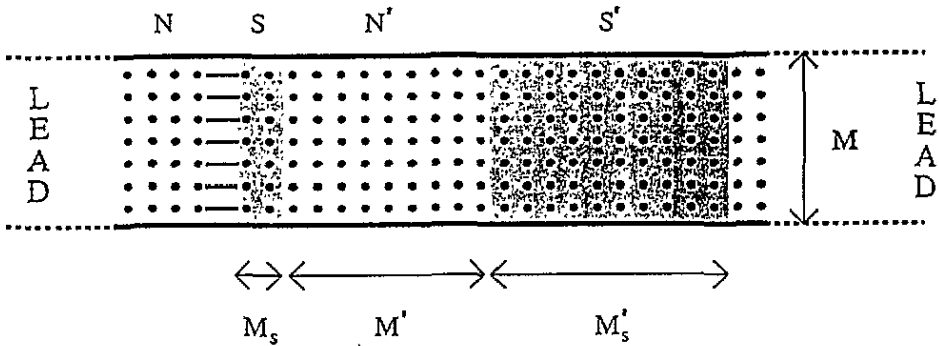


Figure 12. The tight-binding two-dimensional structure used for the N-SS' calculations of figures 13 and 14. The shaded regions denote a superconducting region S of length  $M_S$  sites and another region  $S'$  of length  $M'_S$  sites each of which has on-site order parameter magnitude  $\Delta_0 = 1$ .  $M'_S$  is chosen to give zero quasi-particle transmission through the right-hand superconductor. The left-hand lead is attached to S by hopping elements  $v_L = 0.3$ . All other hopping elements are of magnitude unity.

to be much longer than the superconducting coherence length, so that there is no sub-gap quasi-particle transmission and therefore the sub-gap differential conductance, measured between the right-hand, external, normal lead and  $S'$  is simply the BTK conductance  $2R_a(E)$ . In the limit where the lengths  $M_S, M'_S$  tend to infinity, this structure possesses bound quasi-particle states below the gap [47], which for finite  $M_S$  become transport resonances. In the absence of disorder, there is translational invariance in the transverse direction and therefore transport properties decouple into a superposition of separate resonances, associated with individual open channels.

For a fixed phase of  $\phi = 0$ , figure 13(a) shows a plot of  $R_a(E)$  as a function of  $E/\Delta_0$

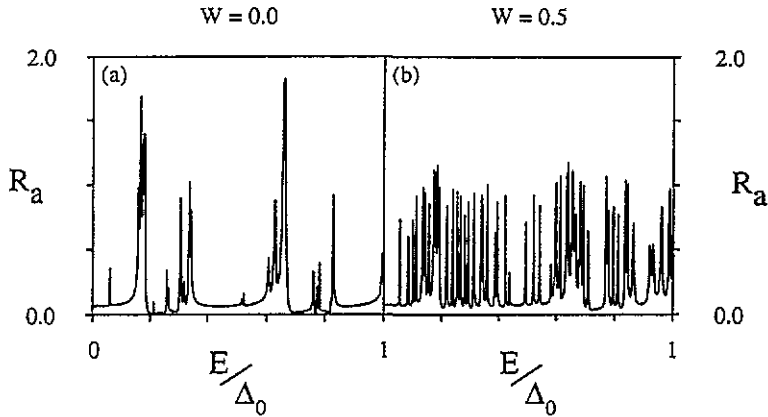


Figure 13. For the structure in figure 12 this figure shows the Andreev reflection coefficient as a function of energy  $E$  for a clean system (a) and a system with disorder  $W = 0.5$  (b).

for a clean system with  $W = 0$ ,  $M = 11$ ,  $M_S = 2$ ,  $M' = 10$ ,  $M'_S = 20$  and  $\Delta_0 = 1$ . To obtain conductance resonances of finite amplitude, it is necessary that an approximate sum rule is broken [46] and, therefore, to introduce some normal scattering, a value of  $v_L = 0.3$  was chosen for the coupling between the left-hand lead and S. Figure 13(b) shows the corresponding plot for a weakly disordered system with disorder  $W = 0.5$ , corresponding to an elastic mean free path of  $l_e = 10.5$ . The analysis of section 6 predicts that the spectra of figure 13 are oscillatory functions of  $\phi$  and, therefore, for a fixed energy  $E$ , phase-periodic resonances appear in the differential conductance. For a clean system, figures 14(a)–(c) show the variation of  $R_a(E)$  with the phase difference  $\phi$ , at energies of  $E = 0$ ,  $\Delta_0/20$  and  $\Delta_0/10$ . Figures 14(d)–(f) show corresponding results in the presence of disorder  $W = 0.5$ .

It should be noted that a naïve picture based on results for a clean structure can be misleading. For example, calculations of bound states between two superconductors of infinite extent [47] predict that at  $\phi = \pi$  a state should pass through zero energy. However, in the presence of normal scattering, which breaks translational symmetry in the longitudinal direction, this feature is no longer present and, in contrast with the case of N–NDOT–S structures of section 6, where the S is only weakly coupled to the NDOT, here zero-voltage conductance resonances are absent.

## 8. Conclusions

We have presented a theoretical framework and general formulae for resonant transport through three classes of hybrid normal–superconducting nanostructures. Results obtained for N–SDOT–N structures demonstrate that if the normal structure is on-resonance at zero energy, then switching on  $\Delta_0$  will typically decrease the conductance of the system. On the other hand, anomalous positive changes in the conductance can occur with a probability proportional to  $\Sigma/\delta\epsilon \sim N(0)v^2/\delta\epsilon$ , where  $v$  is the coupling to the dot,  $\delta\epsilon$  the level spacing and  $N(0)$  is the density of states per site in the normal leads. For applied voltages greater than  $\Delta_0$ , the change in conductance depends on the choice of energy and the precise realization of the impurity potential.

For N–NDOT–S structures, the zero-voltage results of [10] are reproduced. More generally we predict that finite-voltage resonances are almost completely suppressed by

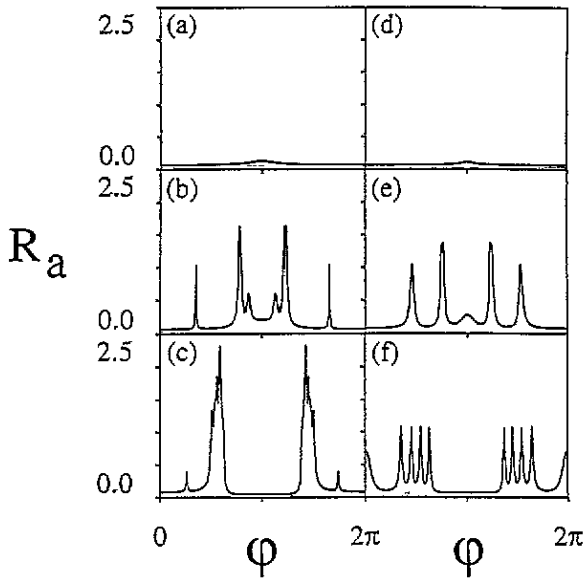


Figure 14. For a clean system (a)–(c) show the variation of  $R_a(E)$  with the phase difference  $\phi$ , at energies of  $E = 0$ ,  $\Delta_0/20$  and  $\Delta_0/10$ ; (d)–(f) show corresponding results in the presence of disorder  $W = 0.5$ .

the switching on of superconductivity and those that survive can have a double-peaked line-shape. This situation can arise at voltages much smaller than the superconducting energy gap, because for a chaotic dot, differential transport at a voltage of the order of the level spacing is sufficient to break particle–hole symmetry. In the analysis of [11], a model containing only a single resonant level was analysed and therefore this feature is absent. Such non-Lorentzian resonances have been discussed in other contexts [48] and may generate non-exponential delay-time curves. This destruction of resonances implies that the typical conductance is large at zero voltage and decreases with increasing bias. This is reminiscent of zero-bias anomalies observed in the sub-gap conductance of superconducting–semiconducting junctions [49, 50], although the theory of such structures [51–54] is rather different from that of section 5.

In section 6 we predicted that a resonant SEQUIN can possess Lorentzian resonances on a scale much smaller than a flux quantum, which suggests that these may provide a new class of magnetometers with a sensitivity at least matching that of present-day SQUIDs. Finally, in section 7, we presented numerical results confirming the above predictions.

### Acknowledgments

This work is supported by the EPSRC, the EC HCM programme, the MOD, the Institute for Scientific Interchange and NATO. We wish to thank Vladimir Prigodin for detailed discussions.

### Appendix A. Current–voltage relations at finite voltages

In the presence of Andreev scattering, current–voltage relations for a phase-coherent scatterer connected only to normal reservoirs were written down in [31]. Although

these have been extended and re-derived in several papers [32, 33, 38], there exists no comprehensive discussion of multi-channel, *finite-voltage* differential conductances. Since such measurements play a central role in studies of resonant structures, we begin with a brief discussion of finite-voltage transport. We also take this opportunity to demonstrate that the finite-temperature analysis of [31, 32] can be applied when superconducting leads with open channels are present.

In the absence of inelastic scattering, dc transport is determined by the quantum mechanical scattering matrix  $s(E, H)$ , which yields scattering properties at energy  $E$  of a phase-coherent structure described by a Hamiltonian  $H$ . If the structure is connected to external reservoirs by open scattering channels labelled by quantum numbers  $n$ , then this has matrix elements of the form  $s_{n,n'}(E, H)$ . The squared modulus of  $s_{n,n'}(E, H)$  is the outgoing flux of quasi-particles along channel  $n$ , arising from a unit incident flux along channel  $n'$ . In what follows, we consider channels belonging to current-carrying leads, with quasi-particles labelled by a discrete quantum number  $\alpha$  ( $\alpha = +1$  for particles,  $-1$  for holes) and therefore write  $n = (l, \alpha)$ , where  $l$  labels all other quantum numbers associated with the leads. With this notation, the scattering matrix elements  $s_{n,n'}(E, H) = s_{l,l'}^{\alpha,\beta}(E, H)$  satisfy  $s^\dagger(E, H) = s^{-1}(E, H)$ ,  $s^\dagger(E, H) = s(E, H^*)$  and if  $E$  is measured relative to the condensate chemical potential  $\mu = e\nu$ ,  $s_{l,l'}^{\alpha,\beta}(E, H) = \alpha\beta[s_{l',l}^{-\alpha,-\beta}(-E, H)]^*$ . For a scatterer connected to external reservoirs by  $L$  crystalline, normal leads, labelled  $i = 1, 2, \dots, L$ , it is convenient to write  $l = (i, a)$ ,  $l' = (j, b)$ , where  $a$  ( $b$ ) is a channel belonging to lead  $i$  ( $j$ ). In addition to those channels belonging to normal leads, there may exist open channels belonging to superconducting leads. To avoid time-dependent order parameter phases varying at the Josephson frequency, which would render a time-independent scattering approach invalid, we insist that all superconductors share a common condensate chemical potential  $\mu$ . For this reason, it is convenient to attach a common label  $l = (0, a)$  to any open channels belonging to the superconductors. In what follows, we focus attention on the quantity

$$P_{i,j}^{\alpha,\beta}(E, H) = \sum_{a,b} |s_{(i,a),(j,b)}^{\alpha,\beta}(E, H)|^2$$

which is the probability of reflection ( $i = j$ ) or transmission ( $i \neq j$ ) of a quasi-particle of type  $\beta$  in lead  $j$  to a quasi-particle of type  $\alpha$  in lead  $i$ . For  $\alpha \neq \beta$ ,  $P_{i,j}^{\alpha,\beta}(E, H)$  is referred to as an Andreev scattering probability, while for  $\alpha = \beta$ , it is a normal scattering probability. Since unitarity yields

$$\sum_{\beta j} |s_{(i,a),(j,b)}^{\alpha,\beta}(E, H)|^2 = \sum_{\alpha a j} |s_{(i,a),(j,b)}^{\alpha,\beta}(E, H)|^2 = 1$$

where  $i$  and  $j$  sum only over leads containing open channels of energy  $E$ , this satisfies

$$\sum_{\beta j=0}^L P_{ij}^{\alpha,\beta}(E, H) = N_i^\alpha(E) \quad \sum_{\alpha i=0}^L P_{ij}^{\alpha,\beta}(E, H) = N_j^\beta(E) \quad (\text{A1})$$

where  $N_i^\alpha(E)$  is the number of open channels for  $\alpha$ -type quasi-particles of energy  $E$  in lead  $i$  satisfying  $N_i^+(E) = N_i^-(-E)$ . For convenience, if a lead  $i$  contains no open channels of energy  $E$ , we have defined  $P_{ij}^{\alpha,\beta}(E, H) = P_{ji}^{\alpha,\beta}(E, H) = 0$  and in equation (A1) summed over all  $i$  and  $j$ .

In the absence of open channels in the superconductor, current-voltage relations at finite voltages and temperatures were derived in [31, 32]. For a system connected by normal leads

to external reservoirs at potentials  $v_i$ ,  $i = 1, 2, \dots, L$ , the current  $I_i$  flowing in a normal lead  $i$  is

$$I_i = \sum_{j=0}^L \bar{A}_{ij} \quad (i = 1, 2, \dots, L) \quad (\text{A2})$$

where

$$\begin{aligned} \bar{A}_{i,j \neq i} &= (2e/h) \sum_{\alpha\beta} (-\alpha) \int_0^\infty dE P_{ij}^{\alpha\beta}(E, H) f_j^\beta(E) \\ \bar{A}_{ii} &= (2e/h) \sum_{\alpha} (\alpha) \left[ \int_0^\infty dE \left\{ N_i^\alpha(E) f_i^\alpha(E) - \sum_{\beta} P_{ii}^{\alpha\beta}(E, H) f_i^\beta(E) \right\} \right] \end{aligned}$$

and  $f_j^\alpha(E) = \{\exp[(E - \alpha(ev_j - \mu))/k_b T] + 1\}^{-1}$  is the distribution of incoming  $\alpha$ -type quasi-particles from lead  $j$ .

Once the currents in the normal leads are known, the current  $I_0$  flowing into the superconductor(s) is given by  $I_0 + \sum_{i=1}^L I_i = 0$ , which allows us to avoid explicitly computing currents in the superconducting regions. For  $i \neq 0$ , the term  $A_{i0}$ , which describes the scattering of quasi-particles originating from the superconductor, takes the form

$$\bar{A}_{i0} = (2e/h) \sum_{\alpha\beta} (-\alpha) \int_0^\infty dE P_{i0}^{\alpha\beta}(E, H) f_0(E)$$

where  $f_0(E) = \{\exp[E/k_b T] + 1\}^{-1}$ . In view of equation (A1), this can be written as

$$\bar{A}_{i0} = (2e/h) \sum_{\alpha} (-\alpha) \int_0^\infty dE \left\{ N_i^\alpha(E) - \sum_{\beta} \sum_{j=1}^L P_{ij}^{\alpha\beta}(E, H) \right\} f_0(E).$$

Hence equation (A2) becomes

$$I_i = \sum_{j=1}^L A_{ij} \quad (\text{A3})$$

where

$$A_{i,j \neq i} = (2e/h) \sum_{\alpha\beta} (-\alpha) \int_0^\infty dE P_{ij}^{\alpha\beta}(E, H) [f_j^\beta(E) - f_0(E)] \quad (\text{A4a})$$

and

$$A_{ii} = (2e/h) \sum_{\alpha} (\alpha) \int_0^\infty dE \{ N_i^\alpha(E) [f_i^\alpha(E) - f_0(E)] - \sum_{\beta} P_{ii}^{\alpha\beta}(E, H) [f_i^\beta(E) - f_0(E)] \}. \quad (\text{A4b})$$

In the zero-temperature limit, these reduce to

$$A_{i,j \neq i} = (2e/h) \int_0^{(ev_j - \mu)} dE \{ P_{ij}^{-+}(E, H) - P_{ij}^{++}(E, H) \} \quad (\text{A5a})$$

$$A_{ii} = (2e/h) \int_0^{(ev_i - \mu)} dE [N_i^+(E) + P_{ii}^{-+}(E, H) - P_{ii}^{++}(E, H)] \quad (\text{A5b})$$

Equations (A4) and (A5) express the coefficients  $A_{ij}$  in terms of scattering matrix elements between normal leads only. Identical equations are derived in the work of [31, 32], which differs from the present analysis by omitting the terms  $i = 0, j = 0$  in equations (A1). For a system connected to normal leads only, these terms are absent. They can also be omitted in the presence of superconducting leads, provided both  $|ev_j - \mu| < \Delta_0$  and  $k_B T < \Delta_0$ , because for energies less than the superconducting energy gap  $\Delta_0$ , there are no open channels in the superconductors.

Equation (A3) yields the current-voltage characteristics of a given structure at finite voltages, provided all scattering coefficients are computed in the presence of a self-consistently determined order parameter. Such calculations have been carried out recently for one-dimensional structures [39, 40] and demonstrate that, provided the currents are low enough, the matrix  $a_{ij}$  can remain unchanged, even on the application of finite voltages of order  $\Delta_0$ . In this limit, the differential of equation (A3) takes the form

$$\delta I_i = \sum_{j=1}^L a_{ij} (\delta v_j - \delta v) \quad (\text{A6})$$

which yields the change in current  $\delta I_i$  due to a change  $\delta E_i$ , where  $E_i = ev_i - \mu$ . At finite temperature,

$$a_{i,j \neq i} = (2e^2/h) \sum_{\alpha\beta} (-\alpha) \int_0^\infty dE P_{ij}^{\alpha\beta}(E, H) \left[ -\beta \frac{\partial f_j^\beta(E)}{\partial E} \right] \quad (\text{A7a})$$

and

$$a_{ii} = (2e^2/h) \sum_{\alpha} (\alpha) \int_0^\infty dE \left\{ N_i^\alpha(E) \left[ -\alpha \frac{\partial f_i^\alpha(E)}{\partial E} \right] - \sum_{\beta} P_{ii}^{\alpha\beta}(E, H) \left[ -\beta \frac{\partial f_i^\beta(E)}{\partial E} \right] \right\}. \quad (\text{A7b})$$

At zero temperature, after taking advantage of particle-hole symmetry, these reduce to (in units of  $2e^2/h$ )

$$a_{i,j \neq i} = P_{ij}^{-+}(E_j, H) - P_{ij}^{++}(E_j, H) \quad (\text{A7c})$$

and

$$a_{ii} = N_i^+(E_i) + P_{ii}^{-+}(E_i, H) - P_{ii}^{++}(E_i, H). \quad (\text{A7d})$$

In the limit  $\{E_i\} \rightarrow 0$ , combining these expressions with the  $s$ -matrix symmetries stated at the beginning of this section, yields the reciprocity relation  $a_{ij}(H) = a_{ji}(H^*)$  [41].

Starting from the above results, expressions for a variety of transport coefficients can be derived. For example in the presence of one normal lead, where the matrix  $A$  reduces to a single number, one finds  $I_1 = A_{11}$ , and from equation (A6), for the differential conductance  $G(E_1) = dI_1/d(v_1 - v) = a_{11}$ . This equation, which at zero temperature reduces to

$$G(E_1) = a_{11} = N_1^+(E_1) + P_{11}^{-+}(E_1, H) - P_{11}^{++}(E_1, H) \quad (\text{A8})$$

was first derived by Blonder, Tinkham and Klapwijk (BTK) [14] in the presence of a single, well-defined boundary between the normal scatterer and superconductor. More generally, the above discussion shows that equation (A8) is valid even if there exist many distinct superconducting regions, provided all superconductors possess a common condensate potential. Thus equation (A8) is more than a simple boundary conductance formula and applies to any phase-coherent system connected to a single normal reservoir.

If the superconductor contains no open channels at energy  $E_1$ , then equation (A1) yields  $N_1^+(E_1) = P_{11}^{-+}(E_1, H) + P_{11}^{++}(E_1, H)$  and therefore

$$G(E_1) = 2P_{11}^{-+}(E_1, H). \quad (\text{A9})$$

In the presence of two normal leads, equation (A6) yields

$$\begin{pmatrix} \delta v_1 - \delta v \\ \delta v_2 - \delta v \end{pmatrix} = \frac{1}{d} \begin{pmatrix} a_{22} & -a_{12} \\ -a_{21} & a_{11} \end{pmatrix} \begin{pmatrix} \delta I_1 \\ \delta I_2 \end{pmatrix} \quad (\text{A10})$$

where  $d = a_{11}a_{22} - a_{12}a_{21}$ . If the superconductor carries no current, then in contrast with a BTK conductance measurement, in which the condensate potential  $\mu$  is fixed by the superconducting contact,  $\mu$  must now be determined via the condition

$$\begin{pmatrix} \delta I_1 \\ \delta I_2 \end{pmatrix} = \begin{pmatrix} \delta I \\ -\delta I \end{pmatrix}.$$

Hence the two-probe conductance  $G = \delta I / (\delta v_1 - \delta v_2)$  takes the form

$$G = \frac{d}{a_{11} + a_{22} + a_{12} + a_{21}}. \quad (\text{A11})$$

The right-hand side of this expression can be evaluated once the energies  $E_1$  and  $E_2$  are known. In the zero-voltage limit  $E_1 = E_2 = 0$ , where all quantities are evaluated at zero energy, equation (A11) can be written [18, 31, 32] as

$$G = T_0 + T_a + \frac{2(R_a R'_a - T_a T'_a)}{R_a + R'_a + T_a + T'_a} \quad (\text{A12})$$

where  $R_0 = P_{11}^{++}(0, H)$ ,  $T_0 = P_{21}^{++}(0, H)$  ( $R_a = P_{11}^{-+}(0, H)$ ,  $T_a = P_{21}^{-+}(0, H)$ ) are probabilities for normal (Andreev) reflection and transmission for quasi-particles from reservoir 1, while  $R'_0, T'_0$  ( $R'_a, T'_a$ ) are corresponding probabilities for quasi-particles from reservoir 2. In the presence of  $N = N_1^+(0) = N_2^+(0)$  open channels per lead, equations (A1) yield  $R_0 + T_0 + R_a + T_a = R'_0 + T'_0 + R'_a + T'_a = N$  and  $T_0 + T_a = T'_0 + T'_a$ .

If the superconductor is able to carry a steady-state current (i.e. if part of the superconductor forms an external lead), then an alternative transport measurement is obtained by setting the current in one of the normal leads to zero. If this lead is labelled  $j$  and the other normal lead labelled  $i$  then, since  $\delta I_j = 0$ , equation (A10) yields  $\delta I_i = G_i(\delta v_i - \delta v)$ , where

$$G_i = d/a_{jj}. \quad (\text{A14})$$

Furthermore,  $\delta v_j - \delta v = \bar{G}_i(\delta v_i - \delta v)$ , where

$$\bar{G}_i = \frac{-a_{ji}}{a_{jj}}. \quad (\text{A15})$$

Since  $a_{ij}$  can have arbitrary sign, the sign of  $\delta v_j - \delta v$  relative to  $\delta v_i - \delta v$  is not fixed.

At finite voltages, the energies  $E_i$  to be used in evaluating the coefficients of (A11) are determined by the requirement  $I_1 = I_2$ , which yields

$$A_{11} + A_{22} + A_{12} + A_{21} = 0. \quad (\text{A16})$$

Similarly the energies to be used in (A14) and (A15) are determined by the requirement  $I_j = 0$ , which yields

$$A_{j1} + A_{j2} = 0. \quad (\text{A17})$$

These self-consistency conditions involve integrals over all incident quasi-particle energies and require a knowledge of the  $s$ -matrix over a range of  $E$ . For certain simple structures,  $\mu$  may be determined by symmetry arguments. Otherwise the task of solving these equations is non-trivial.

In practice, if the potential differences  $\delta E_i/e$  can be measured experimentally, the problem of solving these integral equations can be avoided. This will be the case in experiments where the normal reservoir potentials are measured relative to the condensate potential and therefore at least one superconducting lead is present. In such an experiment, the individual coefficients  $a_{ij} = e \delta I_i / \delta E_j$  are measurable and the finite-energy analysis is considerably simplified.

## References

- [1] Kirk W P and Reed M A (ed) 1992 *Nanostructures and Mesoscopic Systems* (San Diego, CA: Academic)
- [2] Kastner M A 1992 *Rev. Mod. Phys.* **64** 849
- [3] Grabert H and Devoret M (ed) 1992 *Single Charge Tunnelling* (New York: Plenum)
- [4] Prigodin V N, Efetov K B and Iida S 1993 *Phys. Rev. Lett.* **71** 1230
- [5] Baranger H U and Mello P A 1994 *Phys. Rev. Lett.* **73** 142
- [6] Jalabert R A, Pichard J-L and Beenakker C W J 1994 *Europhys. Lett.* **27** 255
- [7] Fromhold T M, Leadbeater M L, Eaves L, Foster T J, Main P C and Sheard F W 1994 *Surf. Sci.* **305** 511
- [8] Eiles T M, Martinis J M and Devoret M H 1993 *Phys. Rev. Lett.* **70** 1862
- [9] Hekking F W J, Glazman L I, Matveev K A and Shekter R I 1993 *Phys. Rev. Lett.* **70** 4138
- [10] Beenakker C W J 1992 *Phys. Rev. B* **46** 12 841
- [11] Khlus V A, Dyomin A V and Zazunov A L 1994 *Physica C* **214** 413–25
- [12] Breit G and Wigner E P 1936 *Phys. Rev.* **49** 519
- [13] Landau L D and Lifshitz E M 1977 *Quantum Mechanics (Non-relativistic Theory)* (Oxford: Pergamon) p 603
- [14] Blonder G E, Tinkham M and Klapwijk T M 1982 *Phys. Rev. B* **25** 4515
- [15] Al'tshuler B L and Spivak B Z 1987 *Sov. Phys.-JETP* **65** 343
- [16] Nakano H and Takayanagi H 1991 *Solid State Commun.* **80** 997
- [17] Takagi S 1992 *Solid State Commun.* **81** 579
- [18] Lambert C J 1993 *J. Phys.: Condens. Matter* **5** 707
- [19] Hui V C and Lambert C J 1993 *Europhys. Lett.* **23** 203
- [20] Hekking F W J and Nazarov Yu V 1993 *Phys. Rev. Lett.* **71** 1625
- [21] Nazarov Yu V 1994 *Phys. Rev. Lett.* **73** 1420
- [22] Zaitsev A V 1994 *Phys. Lett.* **194A** 315
- [23] van Wees B J, Dimoulas A, Heida J P, Klapwijk T M, van der Graaf W and Borghs G 1994 *Physica B* **203** 285
- [24] de Vegvar P G N, Fulton T A, Mallison W H and Miller R E 1994 *Phys. Rev. Lett.* **73** 1416
- [25] Pothier H, Gueron S, Esteve D, and Devoret M H 1994 *Physica B* **203** 226
- [26] Petrashov V T, Antonov V N, Maksimov S V and Shaikhaidarov R Sh 1994 *JETP Lett.* **59** 551
- [27] Hui V C and Lambert C J 1993 *J. Phys.: Condens. Matter* **5** L651
- [28] Hui V C and Lambert C J 1994 *Physica B* **194–196** 1673

- [29] Petrashov V T and Antonov V N 1991 *JETP Lett.* **54** 241
- [30] Petrashov V T, Antonov V N, Maksimov S V and Shaikhaidarov R Sh 1993 *JETP Lett.* **58** 49
- [31] Lambert C J 1991 *J. Phys.: Condens. Matter* **3** 6579
- [32] Lambert C J, Hui V C and Robinson S J 1993 *J. Phys.: Condens. Matter* **5** 4187
- [33] Lambert C J 1994 *Physica B* **203** 201
- [34] Farusaki A, Takayanagi H and Tsukada M 1991 *Phys. Rev. Lett.* **67** 132
- [35] Beenakker C W J and van Houten H 1991 *Phys. Rev. Lett.* **66** 3056
- [36] Bagwell P F 1992 *Phys. Rev. B* **46** 12,573
- [37] Lambert C J and Martin A 1994 *J. Phys.: Condens. Matter* **6** L221
- [38] Takane Y and Ebisawa H 1992 *J. Phys. Soc. Japan* **61** 1685
- [39] Martin A and Lambert C J 1995 *Phys. Rev. B* **51** 17999
- [40] Sols F and Sanchez-Canizares J 1995 *J. Phys.: Condens. Matter* **7** L317
- [41] For a discussion of reciprocity in normal systems, see Büttiker M 1988 *IBM J. Res. Dev.* **32** 317
- [42] Büttiker M, Imry Y and Azbel M Ya 1982 *Phys. Rev. A* **30** 1982
- [43] Büttiker M 1988 *Phys. Rev. B* **38** 12724
- [44] Nöckel J U and Stone A D 1995 *Phys. Rev. B* **50** 17415
- [45] Büttiker M 1988 *IBM J. Res. Dev.* **32** 63
- [46] Cook P, Hui V C and Lambert C J 1995 *Europhys. Lett.* **30** 355
- [47] Kulik I O 1970 *Sov. Phys.-JETP* **30** 944
- [48] Goldberger M L and Watson K M 1964 *Phys. Rev.* **136** B1472
- [49] Kastalasky A, Kleinsasser A W, Greene L H, Bhat R and Harbison J P 1991 *Phys. Rev. Lett.* **67** 3026
- [50] van Wees B J, de Vries P, Magnee P and Klapwijk T M 1992 *Phys. Rev. Lett.* **69** 510
- [51] Zaitsev A V 1990 *JETP Lett.* **51** 41
- [52] Volkov A F and Klapwijk T M 1992 *Phys. Lett.* **168A** 217
- [53] Volkov A F, Zaitsev A V and Klapwijk T M 1993 *Physica C* **210** 217
- [54] Marmakos I K, Beenakker C W J and Jalabert R A 1993 *Phys. Rev. B* **48** 2811